International Journal of Applied Mathematics

Volume 38 No. 11s, 2025
ISSN: 1311-1728 (printed version); ISSN: 1314-8060 (on-line version)

MODELİNG AND ANALYSİS OF THE FRACTİONAL-ORDER *SIRC* EPİDEMİC SYSTEM WİTH TREATMENT SURVİVAL RATE

Devipriya G[1], Sudha D[1,*]

[1] *Departmenet of Mathematics, Sri Krishna Adithya College of Arts & Science, Coimbatore-641042, Tamil Nadu, India*

Abstract

This study proposes a fractional-order Susceptible–Infected–Recovered–Cross-Immune ($SIRC$) epidemic model that incorporates both therapeutic cure rate and cross-immunity effects to better represent viral infection dynamics in human populations. The model is formulated using the Caputo–Fabrizio fractional derivative, which effectively captures memory and hereditary properties without singular kernels. An analytical approximation of the model is derived through the Homotopy Analysis Method (HAM), providing a rapidly convergent series solution with explicit convergence control via h-curves. Numerical simulations validate the efficiency and accuracy of the method, showing that an accurate approximation can be achieved with only six terms of the series expansion. The proposed framework demonstrates the significance of incorporating both treatment interventions and partial immunity in understanding epidemic behavior. The combined use of HAM and the Caputo–Fabrizio derivative establishes a reliable and computationally efficient approach for analyzing complex infectious disease dynamics influenced by memory effects.

Keywords: Fractional epidemic model, Caputo–Fabrizio derivative, Homotopy Analysis Method, Cross-immunity, Therapeutic cure rate, h-curve, Numerical analysis.

1. INTRODUCTION

A significant health concern has emerged due to the extensive spread of infectious diseases among many individuals. Infections tend to claim the lives of a sizable section of the world's population. Mathematical modelling of epidemics, including virus dynamics, can be utilised to reduce the risks of epidemic infections. To comprehend the nature of virally induced infectious illnesses, like the coronavirus, hepadnavirus, and hepacivirus, a number of mathematical models have been developed [1, 2]. The nomenclature Susceptible-Infected-Recovered ($\boldsymbol{SIR}$), which was developed by the ground breaking work of [7], defined the early epidemiological research that described the relationship between the three compartments [3-6]. These early mathematical models then serve as the foundation for models of outbreaks. The incidence rate is regarded as a critical component by experts who explore the evolution of transmissible diseases. That rate may state the number of new infection cases over a specific time period. A kind of propagation prevalence rate referred to as the bilinear outbreak rate has been used in many mathematical biological models, as the bilinear incidence function typically describes the rate of illness dispersion [8-10]. To accurately describe biological processes mathematically, many biological aspects of the human body must be taken into account.

Received: August 05, 2025

Volume 38 No. 11s, 2025
ISSN: 1311-1728 (printed version); ISSN: 1314-8060 (on-line version)

Several studies have expanded the Kermack and McKendrick model by integrating diverse biological characteristics of the population [11, 12]. More specifically, experts examine how human demographic events such as births and deaths impact population size in [11]. The disease-induced fatality rate and vaccination access are considered by the writers in [12] to help the pandemic. The treatment cure rate is the rate at which an infected person can eventually recover to health. Many literary functions examine systems that are biological and contemplate population trends using a model of an outbreak that takes treatment cure rate into consideration [13-15]. Ordinary differential equations (ODEs) are used in all of the preceding articles to describe the numerical representations of contagious disease transmission. The study of infectious diseases often uses a variety of mathematical model types, notably fractional models. The partial derivative structure consists of a set of non-integer ordering variable calculations. Gottfried Wilhelm Leibniz originally gave this to Guillaume de L'Hopital in a piece of writing. Leibniz enquired as to whether the letter contains the initial half-derivatives, where n = (1/2) [16]. It is possible to identify several types of fractional derivatives, including Caputo, Riemann-Liouville (R-L), Atangana-Baleanu (A-B), and Caputo-Fabrizio (C-F). The ability of fractional-order models to shed light on the influence of memory is one of their main advantages [17-19]. Because of this, fractional computations are used in many domains outside of biology to accurately model real-world issues. These disciplines include mechanics, finance, image processing, engineering, and physics [20]. The authors give multiple instances of fractional derivatives in the actual world in [21], demonstrating that fractional mathematical systems provide a modelling approach that is more accurate than classic integer-based differential calculus. Biologically, memory has been demonstrated to be one of the fundamental characteristics of immune response and cell membranes [22]. We note that in order to demonstrate the properties or behaviour of the human liver, the authors in [23] created a computational framework that includes the C–F fractional derivative. In recent times, several researchers have used fractional order derivative systems (FODs) to extend the simulation of infection rates [24-32]. Better yet, the scientists created and assessed a framework for fractal order in [24], which depicts the dynamics of hepadnavirus illness spreading between hepatocytes. Similarly, [25] describes and investigates the viral dynamics of hepacivirus using fractional differential equations. Scholars have constructed multiple frameworks utilising fractional derivatives, such as SEIR [26], SEIQR [27] and SEIQR (quarantined) [28], to investigate the impact of memory on the dynamics of the COVID-19 global epidemic within a group of people. [29, 30] presents and evaluates basic SIR fractional-order models for epidemics, taking into account temporal and geographic aspects [29] and media coverage [34]. The authors in [31] propose an arithmetical form of dengue spread in Nepal that incorporates injection and medical care using fractional-order derivatives. Fractional anti-derivatives are a useful tool for simulating epidemic diseases because they generate additional practical outcomes. Our point was illustrated by contrasting the clinical data with the results from fractional calculus and classical calculus [33–35]. The authors in [36] demonstrate that altering the fractal order has a direct impact on the dynamics of cancer cells through the comparison of different ordered fractions and fractal aspect values. A fractional most favourable control trouble was also studied, and the findings show that fractional modelling of the problem offered

Received: August 05, 2025

Volume 38 No. 11s, 2025
ISSN: 1311-1728 (printed version); ISSN: 1314-8060 (on-line version)

a better approximation than the classical approach. [37] Proposes a comparison with a cholera outbreak scenario in the real world. To model biological structures, it has been found that fractional-order differential equations perform better than conventional integer-level differential equations.

The present inquiry stems from the numerous advantages of fractional form mathematical calculations for biological system modelling, as previously discussed. Many recent researchers who have researched three-compartment $\boldsymbol{SIR}$ fractional epidemic models have considered bilinear incidence rates. The global stability of a fractional theory of $\boldsymbol{SIR}$ with three compartments and frequency of incidents, for instance, was investigated by the authors in [38,39] examines an equivalent scenario using the homotopy study method and the Laplace transform. The trio of compartments the fractional model $\boldsymbol{SIR}$ [40] incorporates a continual vaccination method, and the authors have taken into account the bilinear frequency rate to characterise the source of infection. Recently Alzahrani introduced a fractional stochastic $SIRC$ model for salmonella infection dynamics with Caputo formulation to capture randomness and memory effects. This work demonstrated ergodicity, stability, uniqueness, and existence of solutions, as well as numerical validation through the use of the Milstein scheme. These results emphasize how crucial it is to include fractional and stochastic dynamics in order to comprehend the transmission of infectious diseases [40]. The authors in [41] developed fractional-order epidemic $\boldsymbol{SIR}$ –$\boldsymbol{SI}$ epidemic model to evaluate the transmission dynamics of dengue fever. The model is formulated as a system of nonlinear differential equations and is further extended by incorporating fractional order derivatives in the Caputo sense to capture memory effects in disease transmission. The study [42] presented a comprehensive investigation of the fractional SEIR epidemic model to explore the transmission dynamics of infectious diseases. The study employed advanced semi-analytical techniques, namely the Yang Transform Decomposition Method (YTDM) and the Homotopy Perturbation Transform Method (HPTM), which effectively combine the strengths of the Adomian Decomposition Method (ADM), Homotopy Perturbation Method (HPM), and Yang Transform. These hybrid approaches provided rapidly convergent analytical series solutions, demonstrating their efficiency and accuracy in solving nonlinear fractional differential equations that describe epidemic propagation.

In recent years, numerous fractional-order epidemic models have been formulated to account for memory effects and to enhance the realism of disease transmission dynamics. Despite this progress, several critical limitations persist. First, most fractional-order SIR-type frameworks overlook the influence of cross-immunity, even though partial or temporary immunity following recovery is a well-documented phenomenon in epidemics such as COVID-19 and influenza. Second, the therapeutic cure rate, representing the effect of medical interventions on the recovery process, is seldom integrated into fractional epidemic models, thereby limiting their usefulness for practical epidemiological or policy applications. Third, the majority of existing studies employ purely numerical methods without explicit convergence control mechanisms, which can lead to computational inefficiency and instability.

Received: August 05, 2025

Volume 38 No. 11s, 2025
ISSN: 1311-1728 (printed version); ISSN: 1314-8060 (on-line version)

Although the Homotopy Analysis Method (HAM) offers systematic convergence control through h-curves, its potential in fractional epidemic modeling remains largely unexplored. Similarly, the Caputo–Fabrizio derivative, with its non-singular and nonlocal kernel that effectively characterizes memory effects, has rarely been applied to extended epidemic systems that account for cross-immunity and treatment. Furthermore, the efficiency of obtaining accurate analytical approximations with a minimal number of series terms is not well documented, as most methods demand extensive computational effort for high accuracy.

To address these gaps, the present study develops a fractional-order $SIRC$ model that simultaneously incorporates treatment dynamics and cross-immunity within the Caputo–Fabrizio framework. The analytical solution is derived via the Homotopy Analysis Method, which ensures convergence control through h-curves and demonstrates that precise results can be achieved with only a few approximation terms. This unified modeling approach effectively captures the memory characteristics inherent in fractional calculus while maintaining computational efficiency and biological realism in simulating infectious disease dynamics.

The following is the paper's structure: The next part introduces some of the fundamentals of fractional calculus. An examination of several fundamental findings presented in Section 3 is the solution of the $SIRC$ model by the HAM. While Section 4 illustrates worldwide steadiness, Section 5 presents numerical simulations that identify the stability of the steady states and the effect of the therapy cure rate. An overview of the presented work concludes the paper.

2. MOTIVATION AND MATHEMATICAL FORMULATION

Mathematical modelling of infectious illnesses is crucial for understanding transmission patterns and evaluating control approaches. Mathematics and biology experts are driven to analyze and evaluate the dynamical processes affecting these diseases to forecast their longterm dissemination and control. The fundamental criteria of infectious diseases are delineated by four epidemiological categories that assess the susceptible population: the infected, the recovered, and the deceased. The $SIRC$ model is a variation of the conventional $\boldsymbol{SIR}$ model. Isolating sick individuals has proven to be a more efficacious method for halting the transmission of the disease. The dynamics of epidemic models have been analyzed utilizing several types of fractional calculus over the years, including Caputo-Fabrizio [19], Katugampola, Atangana-Baleanu [18]. Each possesses advantages and disadvantages. Zhanget formulated the specific asymptotic stability criteria for time-delayed fractional-order gene regulation systems. Wu et al. investigated global uniform asymptotic stability in fractional-order gene regulatory networks characterized by time-varying delays and structural uncertainty. Zhang et al. proposed a novel stabilization criterion for fractional-order composite systems with time delay, utilizing the vector Lyapunov function. The study has utilized the Caputo–Fabrizio derivative, which possesses a nonlocal and non-singular exponential kernel, as it is deemed most suitable for examining COVID-19 dynamics [30-40]. Inspired by preliminary research, a fractional order $\boldsymbol{SIQR}$ model is employed to delineate the dynamics of COVID-19 transmission and utilize a suitable mathematical framework [$\boldsymbol{SIQR}$ model] to assess the disease's impact within the context of the Caputo-Fabrizio fractional differential

Received: August 05, 2025

Volume 38 No. 11s, 2025
ISSN: 1311-1728 (printed version); ISSN: 1314-8060 (on-line version)

equation. To analyze the situation of an epidemic characterized by Susceptible, Infected, Recovered, and Cross Immune $SIRC$. Several critical assumptions are established to formulate the $SIRC$ disease transmission model. At each given time t ≥ 0, the population N is categorized into four classes: Susceptible individuals S, Infected individuals I, Recovered individuals R, and Cross-immune individuals C. Currently, $N(\tau) = S(\tau) + I(\tau) + R(\tau) + C(\tau)$. In this framework, those at risk of acquiring an infection are deemed susceptible. An infected individual exhibiting symptoms of the sickness and isolated is considered recovered. Individuals that possess cross-immunity and recuperate from the sickness are designated as Recovered. The subsequent fractional order differential equations are given as:

$$\begin{cases} x\alpha DS(\tau) = \varphi(1-S) - \phi SI + \delta \\ x\alpha DI(\tau) = \varphi SI + \eta\varphi CI - (\chi+\phi)I \end{cases} \quad \begin{cases} x\alpha DR(\tau) = (1-\eta)\varphi CI + \alpha I - (\chi+\phi)R \\ x\alpha DC(\tau) = -\varphi CI - (\delta+\chi)C + \phi R \end{cases} \tag{1}$$

Table 1: Interpretation of parameters and variables

Parameters & Variables	**Meaning**
χ	In each division, the number of deaths is assumed to be equal to the number of infants in the population.
δ	The degree of the cross-immune population's susceptibility
φ	Contact frequency
η	Average likelihood of cross-immune persons re-infecting
ψ	Percentage of the infected population that has recovered.
ϕ	The rate of population recovery from complete immunity to partial immunity and from the cross-immune population
S	Susceptible
I	Infected
R	Recovered
C	Cross-immune

3. PRELIMINARIES

Fractional order derivatives and anti-derivatives can be explained in a variety of ways. Nonetheless, two of the most well-known instances are the Caputo and Riemann-Liouville (R-L) fractional order derivatives.

Definition: 3.1 Riemann-Liouville fractional derivative of order $(\alpha > 0)$ for a real valued function $f(t)$ is given as,

$${}^{\mathrm{RL}}D_a^{\alpha} f(t) = \frac{1}{\Gamma(n-\alpha)} \frac{d^n}{dt^n} \int_a^t \frac{f(\tau)}{(t-\tau)^{\alpha-n+1}} d\tau, \ (n-1) < \alpha < n;\ n \in N\left(\frac{d^n}{dt^n}\right) f(t), \ \alpha = n \in N$$

Definition: 3.2 Caputo fractional derivative of order$\alpha > 0$ for a real valued function is,

International Journal of Applied Mathematics
Volume 38 No. 11s, 2025
ISSN: 1311-1728 (printed version); ISSN: 1314-8060 (on-line version)

$${}^{C}D_a^{\alpha} f(t) = \frac{1}{\Gamma(n-\alpha)} \int_a^t \frac{f^n(\tau)}{(t-\tau)^{\alpha-n+1}} d\tau, n-1 < \alpha < n; n \in N \frac{d^n}{dt^n} f(t),\ \alpha = n \in N$$

Definition: 3.3 Let u be a function in $H^{\alpha}(a,b), (b > a)$at $0 < \alpha < 1$ then, the new Caputo-Fabrizio derivative of fractional order α is

$${}^{CF}D_t^{\alpha} u(x,t) = \frac{M(\alpha)}{1-\alpha} \int_0^t \frac{\partial}{\partial \tau} u(x,\tau) exp\left(-\alpha \frac{(t-\tau)}{1-\alpha}\right) d\tau$$

where $M(\alpha)$ is a normalization function satisfying, $M(0) = M(1) = 1$. From [19], we recall that if the function u does not belong to $H^{\alpha}(a;b)$ then, C-F derivative can be written as,

$${}^{CF}D_t^{\alpha} u(x,t) = \frac{\alpha M(\alpha)}{1-\alpha} \int_0^t (u(x,t) - u(x,\tau)) exp\left(-\alpha \frac{(t-\tau)}{1-\alpha}\right) d\tau$$

Definition: 3.4 The fractional integral operator associated to the C-F fractional derivative is expressed as

$${}^{CF}I_t^{\alpha} u(x,t) = \frac{1-\alpha}{M(\alpha)} u(x,t) + \frac{\alpha}{M(\alpha)} \int_0^t u(x,\tau) d\tau$$

It's clear that the Caputo-Fabrizio derivative has no singular kernel, since the kernel is based on exponential function.

Definition: 3.5 Mittag-Leffler function of one parameter α is given as,

$$E_{\alpha}(z) = \sum_{k=0}^{\infty} \left(\frac{z^k}{\Gamma(\alpha k + 1)}\right), Re(\alpha > 0), z \in C.$$

Definition: 3.6 A generalization of Mittag-Leffler functions with two parameters α and β is,

$$E_{\alpha,\beta}(z) = \sum_{k=0}^{\infty} \left(\frac{z^k}{\Gamma(\alpha k + 1)}\right), Re(\alpha > 0), z, \beta \in C.$$

Definition: 3.7 The Hadamard fractional integral (HFI) of order $\alpha > 0$, for a continuous function $\varphi: [1,\infty) \to R$ is defined as,

$${}^{H}J_1^{\alpha} \varphi(t) = \frac{1}{\Gamma(\alpha)} \int_1^t (log \frac{t}{\tau})^{\alpha-1} \varphi(t) \frac{d\tau}{\tau}$$

Definition: 3.8 The Caputa Hadamard fractional integral (CHFI) of order $\alpha > 0$, for a continuous function $\varphi: [1,\infty) \to R$ is defined as,

$${}^{CH}D_1^{\alpha} \varphi(t) = \frac{1}{\Gamma(n-\alpha)} \int_1^t (log \frac{t}{\tau})^{(n-\alpha)-1} \delta^n \varphi(t) \frac{d\tau}{\tau}, (n-1) < \alpha < n$$

Lemma: 3.9 $Let (k,l) > 0$, and $\varphi \epsilon C([a,b],R)$. Then for all $\xi \epsilon [a,b]$, and by assuming $F_a(\xi) = \psi(\xi) = \psi(a)$,

1. $T_a^{k;\psi} T_a^{l;\psi} \varphi(\xi) = T_a^{k+l;\psi} \varphi(\xi)$,
2. $D_a^{k;\psi} T_a^{l;\psi} \varphi(\xi) = \varphi(\xi)$,
3. $T_a^{k;\psi} \left(F_a(\xi)\right)^{l-1} = \frac{\Gamma(l)}{\Gamma(l+k)} \left(F_k(\xi)\right)^{l+q-1}$,

Received: August 05, 2025

International Journal of Applied Mathematics
Volume 38 No. 11s, 2025
ISSN: 1311-1728 (printed version); ISSN: 1314-8060 (on-line version)

4. $D_a^{k;\psi}\left(F_a(\xi)\right)^{l-1} = \frac{\Gamma(l)}{\Gamma(l-q)}\left(F_a(\xi)\right)^{l-k-1}$,
5. $D_a^{k;\psi}\left(F_a(\xi)\right)^{k} = 0$, for $k\,\epsilon\{0,\dots,(n-1)\}, n\epsilon N, k\epsilon((n-1),n)$.

4. ANALYTICAL SOLUTION OF FRACTIONAL *SIRC* EPIDEMIC MODEL BY THE HAM

Let us choose the initial condition for the fractıonal $SIRC$ epıdemıc model as follows:

$S(\tau_0) = s_0 \geq 0,\ I(\tau_0) = i_0 \geq 0,\ R(\tau_0) = r_0 \geq 0,\ C(\tau_0) = c_0 \geq 0$ (2)

The model (1) having fractional order derivatives with the Caputo operator of order $(0 < \alpha \leq 1)$ have been proposed as follows:

The auxiliary linear operators$l_S, l_I, l_R, l_C$are selected as

$$x\alpha DS(\tau) = l_S(\tau, s)$$

$$x\alpha DI(\tau) = l_I(\tau, s)$$

$$x\alpha DR(\tau) = l_R(\tau, s)$$

$$x\alpha DC(\tau) = l_C(\tau, s)$$

which satisfy the following properties,$l_\alpha(\underline{C}_\alpha) = 0$, Where $\underline{C}_\alpha: \alpha \to [0,1]$ are integral constants.

$$N_1[S_\tau, I_\tau, R_\tau, C_\tau] = x\alpha DS(\tau) - \chi(1-S) + \phi SI - \delta C$$

$$N_2[S_\tau, I_\tau, R_\tau, C_\tau] = x\alpha DI(\tau) - \varphi SI - \eta\varphi CI + (\chi + \phi)I$$

$$N_3[S_\tau, I_\tau, R_\tau, C_\tau] = x\alpha DR(\tau) - (1-\eta)\varphi CI - \alpha I + (\chi + \phi)R$$

$$N_4[S_\tau, I_\tau, R_\tau, C_\tau] = x\alpha DC(\tau) + \varphi SI + (\delta + \chi)C - \phi R$$

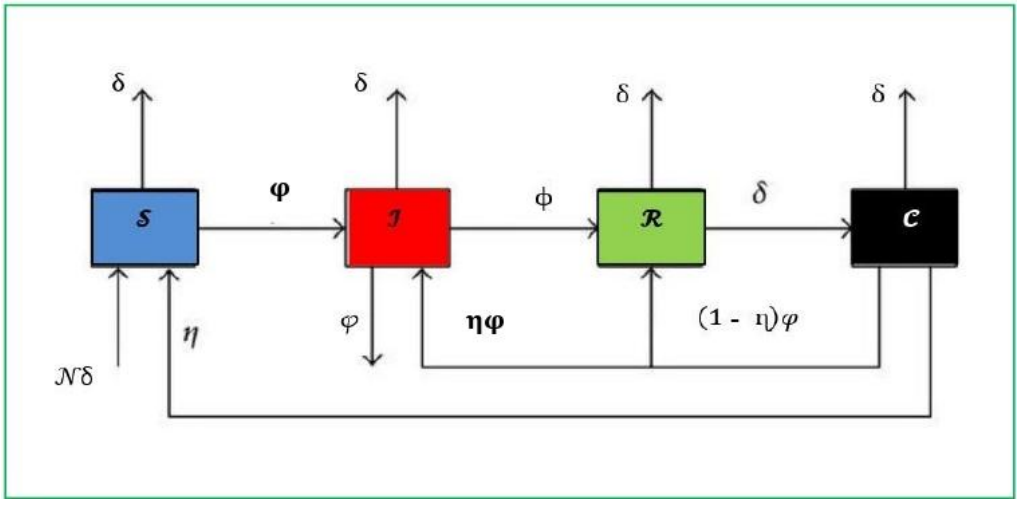

Figure 1: Proposed $SIRC$ Model

Received: August 05, 2025

International Journal of Applied Mathematics
Volume 38 No. 11s, 2025
ISSN: 1311-1728 (printed version); ISSN: 1314-8060 (on-line version)

We generate the zero-order deformation equations using Liao's definitions, apply the not equal to zero auxiliary component $\hbar$ and the not equal to zero auxiliary operation, and find that the embedding parameter is$\Psi(\tau)$: $\mathcal{s}\rightarrow$ [0, 1].

$$(1-s)l_S[S(\tau;s)-S(\tau_0)] = s_0\hbar_S\Psi_S(\tau)n_S[S_\tau,\ I_\tau,\ R_\tau,\ C_\tau] \quad (3)$$

$$(1-s)l_I[I(\tau;s)-I(\tau_0)] = s_0\hbar_I\Psi_I(\tau)n_I[S_\tau,\ I_\tau,\ R_\tau,\ C_\tau] \quad (4)$$

$$(1-s)l_R[R(\tau;s)-R(\tau_0)] = s_0\hbar_R\Psi_R(\tau)n_R[S_\tau,\ I_\tau,\ R_\tau,\ C_\tau] \quad (5)$$

$$(1-s)l_C[C(\tau;s)-C(\tau_0)] = s_0\hbar_C\Psi_C(\tau)n_C[S_\tau,\ I_\tau,\ R_\tau,\ C_\tau] \quad (6)$$

Clearly, when $\mathcal{s}$ = 0 and $\mathcal{s}$ = 1, then

$$S(\tau_0)=s_0,\ I(\tau_0)=i_0,\ R(\tau_0)=r_0, C(\tau_0)=c_0$$

$$S(\tau_1)=s_\tau,\ I(\tau_1)=i_\tau,\ R(\tau_1)=r_\tau,\ C(\tau_1)=c_\tau$$

As a result, the solutions $S(\tau;s)$, $I(\tau;s)$, $R(\tau;s)$, & $C(\tau;s)$ fluctuate continually from $S(\tau_0)$, $I(\tau_0)$, $R(\tau_0)$, & $C(\tau_0)$ to the precise solution $S(\tau_1)$, $I(\tau_1)$, $R(\tau_1)$, & $C(\tau_1)$ when the embed factor increase from 0 → 1. Making use of Taylor's series

$$S(\tau;s) = S(\tau_0) + \sum_{i=1}^{\infty} S_\alpha(\tau_1)s^\alpha \quad (7)$$

$$I(\tau;s) = I(\tau_0) + \sum_{i=1}^{\infty} I_\alpha(\tau_1)s^\alpha \quad (8)$$

$$R(\tau;s) = R(\tau_0) + \sum_{i=1}^{\infty} R_\alpha(\tau_1)s^\alpha \quad (9)$$

$$C(\tau;s) = C(\tau_0) + \sum_{i=1}^{\infty} C_\alpha(\tau_1)s^\alpha \quad (10)$$

The term s^α represents the action of a fractional differential operator, where α is a real number ($0 < \alpha \leq 1$).For each compartment, we introduce the embedding parameters and auxiliary convergence-control parameters as $\Psi(\tau) = \{\Psi_S(\tau), \Psi_I(\tau), \Psi_R(\tau), \Psi_C(\tau)\}$ and $\hbar = \{\hbar_S, \hbar_I, \hbar_R, \hbar_C\}$. Here $\Psi_S(\tau), \Psi_I(\tau), \Psi_R(\tau), \Psi_C(\tau)$ denote the homotopy embedding functions for the Susceptible, Infected, Recovered, and Cross-immune populations, respectively, while $\hbar_S, \hbar_I, \hbar_R, \hbar_C$are the corresponding auxiliary parameters that control the convergence of the HAM series solution for each class. These choices ensure that the solution deforms continuously from the initial guess to the exact solution as τ varies from 0 to 1.

$$S(\tau_1) = S(\tau_0) + \sum_{\alpha=1}^{\infty} S_\alpha(\tau_1)$$

$$I(\tau_1) = I(\tau_0) + \sum_{\alpha=1}^{\infty} I_\alpha(\tau_1)$$

Received: August 05, 2025

International Journal of Applied Mathematics
Volume 38 No. 11s, 2025
ISSN: 1311-1728 (printed version); ISSN: 1314-8060 (on-line version)

$$R(\tau_1) = R(\tau_0) + \sum_{\alpha=1}^{\infty} R_\alpha(\tau_1)$$

$$C(\tau_1) = C(\tau_0) + \sum_{\alpha=1}^{\infty} C_\alpha(\tau_1)$$

where,

$S_\alpha = \frac{1}{i!}\frac{\partial^\alpha(S(\tau;s))}{\partial s^\alpha}|_{s=0},\ I_\alpha = \frac{1}{i!}\frac{\partial^\alpha(I(\tau;s))}{\partial s^\alpha}|_{s=0}, R_\alpha = \frac{1}{i!}\frac{\partial^\alpha(R(\tau;s))}{\partial s^\alpha}|_{s=0}, C_\alpha = \frac{1}{i!}\frac{\partial^\alpha(C(\tau;s))}{\partial s^\alpha}|_{s=0}$

Differentiating (3)–(6) "α" times with respect to s, allocating byα, yields the α-th order deformation equations and putting $\mathcal{s} = 0$.

$$l_S[S_\alpha(\tau_1) - \lambda_\alpha S_{(\alpha-1)}(\tau_1)] = \hbar\underline{\zeta}_{S(\tau_1)}\left(S_{(\alpha-1)}(\tau_1)\right) \quad (11)$$

$$l_I[I_\alpha(\tau_1) - \lambda_\alpha I_{(\alpha-1)}(\tau_1)] = \hbar\underline{\zeta}_{I(\tau_1)}\left(I_{(\alpha-1)}(\tau_1)\right) \quad (12)$$

$$l_R[R_\alpha(\tau_1) - \lambda_\alpha R_{(\alpha-1)}(\tau_1)] = \hbar\underline{\zeta}_{R(\tau_1)}\left(R_{(\alpha-1)}(\tau_1)\right) \quad (13)$$

$$l_C[C_\alpha(\tau_1) - \lambda_\alpha C_{(\alpha-1)}(\tau_1)] = \hbar\underline{\zeta}_{C(\tau_1)}\left(C_{(\alpha-1)}(\tau_1)\right) \quad (14)$$

where,

$$\underline{\zeta}_{S(\tau_1)} = \left(x(\alpha-1)DS(\tau) + \varphi\sum_{j=0}^{(\alpha-1)} S(\tau_j)I(\tau_{\alpha-1-j}) + \chi S(\tau_{(\alpha-1)}) - \delta C_{(\alpha-1)}(\tau_1) - (1-\upsilon)\chi\right)$$

$$\underline{\zeta}_{I(\tau_1)} = \left(x(\alpha-1)DI(\tau) - \varphi\sum_{j=0}^{(\alpha-1)} S(\tau_j)I(\tau_{\alpha-1-j}) - \varphi\eta\sum_{j=0}^{(\alpha-1)} S(\tau_j)I(\tau_{(\alpha-1-j)}) + (\chi+\phi)I(\tau_{(\alpha-1)})\right)$$

Received: August 05, 2025

International Journal of Applied Mathematics
Volume 38 No. 11s, 2025
ISSN: 1311-1728 (printed version); ISSN: 1314-8060 (on-line version)

$$\underline{\zeta}_{R(\tau_1)} = \left(x(\alpha-1)DR(\tau) - (1-\eta)\varphi \sum_{j=0}^{(\alpha-1)} C(\tau_j) I(t_{\alpha-1-j}) + \varphi I(\tau_{\alpha-1}) + (\chi + \phi) R(\tau_{\alpha-1}) \right)$$

$$\underline{\zeta}_{C(\tau_1)} = \left(x(\alpha-1)DC(\tau) + \varphi \sum_{j=0}^{(\alpha-1)} C(\tau_j) I(\tau_{(\alpha-1-j)}) + (\chi+\delta) C(\tau_{(\alpha-1)}) - \phi R(\tau_{(\alpha-1)}) \right)$$

&

$$\lambda_\alpha = \{1, 0, \frac{\alpha > 1}{\alpha \leq 1}$$

When α equals or exceeds 1, the α^{th}-order deformation (11)–(14) turns into

$$S_\alpha(\tau_1) = \lambda_\alpha S_{(\alpha-1)}(\tau_1) + \hbar_\alpha \int_0^t \underline{\zeta}_{S(\tau_1)}(\varsigma) d\varsigma$$

$$I_\alpha(\tau_1) = \lambda_\alpha I_{(\alpha-1)}(\tau_1) + \hbar_\alpha \int_0^t \underline{\zeta}_{I(\tau_1)}(\varsigma) d\varsigma$$

$$R_\alpha(\tau_1) = \lambda_\alpha R_{(\alpha-1)}(\tau_1) + \hbar_\alpha \int_0^t \underline{\zeta}_{R(\tau_1)}(\varsigma) d\varsigma$$

$$C_\alpha(\tau_1) = \lambda_\alpha C_{(\alpha-1)}(\tau_1) + \hbar_\alpha \int_0^t \underline{\zeta}_{C(\tau_1)}(\varsigma) d\varsigma$$

5. NUMERICAL SIMULATIONS

For the numerical simulations, the parameter values are adopted from [41] as follows:

$S(\tau_0) = 0.3, I(\tau_0) = 0.5,\ R(\tau_0) = 0, C(\tau_0) = 0.6,\ \varphi = 1.3, \chi = 0.09, \phi = 0.01, \delta = 0.05, \psi = 0.36,$

$\eta = 0.9.$

Using Taylor's series expansion implemented in Maple, the sixth-order analytical approximation of the model was obtained, as presented below.

Received: August 05, 2025

International Journal of Applied Mathematics
Volume 38 No. 11s, 2025
ISSN: 1311-1728 (printed version); ISSN: 1314-8060 (on-line version)

$$S(\tau_1) = 0.3 + 0.612\hbar\tau + 1.53\hbar^2\tau + 2.04\hbar^3\tau + 1.53\hbar^4\tau + 0.612\hbar^5\tau + 0.602\hbar^6\tau - 0.550575\hbar^2\tau^2 - 1.4682\hbar^3\tau^3 - 1.65173\hbar^4\tau^2 - 0.88092\hbar^5\tau^2 - 0.183525\hbar^6\tau^2 - 0.667932\hbar^3\tau^3 - 1.50285\hbar^4\tau^3 + 1.20228\hbar^5\tau^3 - 0.333966\hbar^6\tau^3 + 0.062761\hbar^4\tau^4 + 0.100427\hbar^5\tau^4 - 0.0418447\hbar^6\tau^4 - 0.0461811\hbar^5\tau^5 - 0.0384842\hbar^6\tau^5 - 0.00050418\hbar^3\tau^3 + \cdots$$

(15)

$$I(\tau_1) = 0.5 - 1.926\hbar\tau - 4.815\hbar^2\tau - 6.42\hbar^3\tau - 4.815\hbar^4\tau - 1.926\hbar^5\tau - 0.321\hbar^6\tau - 1.03131\hbar^2\tau^2 - 2.75016\tau^3 - 3.09393\hbar^4\tau^2 - 1.6501\hbar^5\tau^2 - 0.34377\hbar^6\tau^2 + 1.63923\hbar^3\tau^3 - 3.68826\hbar^4\tau^3 - 2.95061\hbar^5\tau^3 - 0.819613\hbar^6\tau^3 + 0.2508\hbar^4\tau^4 + 0.40128\hbar^5\tau^4 - 0.1672\hbar^6\tau^4 - 0.115992\hbar^5\tau^5 - 0.09666\hbar^6\tau^5 - 0.00467747\hbar^6\tau^6 + \cdots$$

(16)

$$R(\tau_1) = 0.001 - 1.314\hbar\tau - 3.285\hbar^2\tau - 4.38\hbar^3\tau - 3.825\hbar^4\tau - 1.314\hbar^5\tau - 0.219\hbar^6\tau + 0.511335\hbar^2\tau^2 + 1.36356h^3\tau^2 + 1.53401\hbar^4\tau^2 + 0.81813\hbar^5\tau^2 + 0.170445\hbar^6\tau^2 + 0.344179\hbar^3\tau^3 + 0.774402\hbar^4\tau^3 - 0.619522\hbar^5\tau^3 + 0.172089\hbar^6\tau^3 - 0.0790303h^4\tau^4 - 0.0126448\hbar^5\tau^4 - 0.0526868\hbar^6\tau^4 - 0.0173387\hbar^5\tau^5 - 0.0144489\hbar^6\tau^5 + 0.000654392\hbar^6\tau^6 + \cdots$$

(17)

$$C(\tau_1) = 0.6 + 2.844\hbar\tau + 7.11\hbar^2\tau + 9.48\hbar^3\tau + 7.11\hbar^4\tau + 2.844\hbar^5\tau + 0.474\hbar^6\tau + 1.0948\hbar^2\tau^2 + 2.9196h^3\tau^2 + 3.28455\hbar^4\tau^2 + 1.7516\hbar^5\tau^2 + 0.36495\hbar^6\tau^2 - 1.3145\hbar^3\tau^3 - 2.95763\hbar^4\tau^3 - 2.3661\hbar^5\tau^3 - 0.65725\hbar^6\tau^3 - 0.23452h^4\tau^4 - 0.375233\hbar^5\tau^4 - 0.156347\hbar^6\tau^4 + 0.0871498\hbar^5\tau^5 + 0.0726248\hbar^6\tau^5 + 0.00452726\hbar^6\tau^6 + \cdots$$

(18)

6. DISCUSSION

As observed, the solutions derived from equations (11)–(14) involving the auxiliary parameter $\hbar$ illustrate the approach proposed by **Liao**, which enables effective adjustment and control of the convergence of the series solution.

Table.2 shows the values of $\hbar$'s.

$\hbar^*$	Minimum value
$S(\tau_1)$	-1.4≤ $\hbar_1 \leq -0.4$
$I(\tau_1)$	-1.3≤ $\hbar_2 \leq -0.6$
$R(\tau_1)$	-1.3≤ $\hbar_3 \leq -0.6$
$C(\tau_1)$	-1.4≤ $\hbar_4 \leq -0.4$

Received: August 05, 2025

International Journal of Applied Mathematics
Volume 38 No. 11s, 2025
ISSN: 1311-1728 (printed version); ISSN: 1314-8060 (on-line version)

Figure 2 shows the fifth and sixth order approximations of $S(\tau_0), I(\tau_0), R(\tau_0)$ & $C(\tau_0)$ and $S(\tau_1), I(\tau_1), R(\tau_1)$ & $C(\tau_1)$.

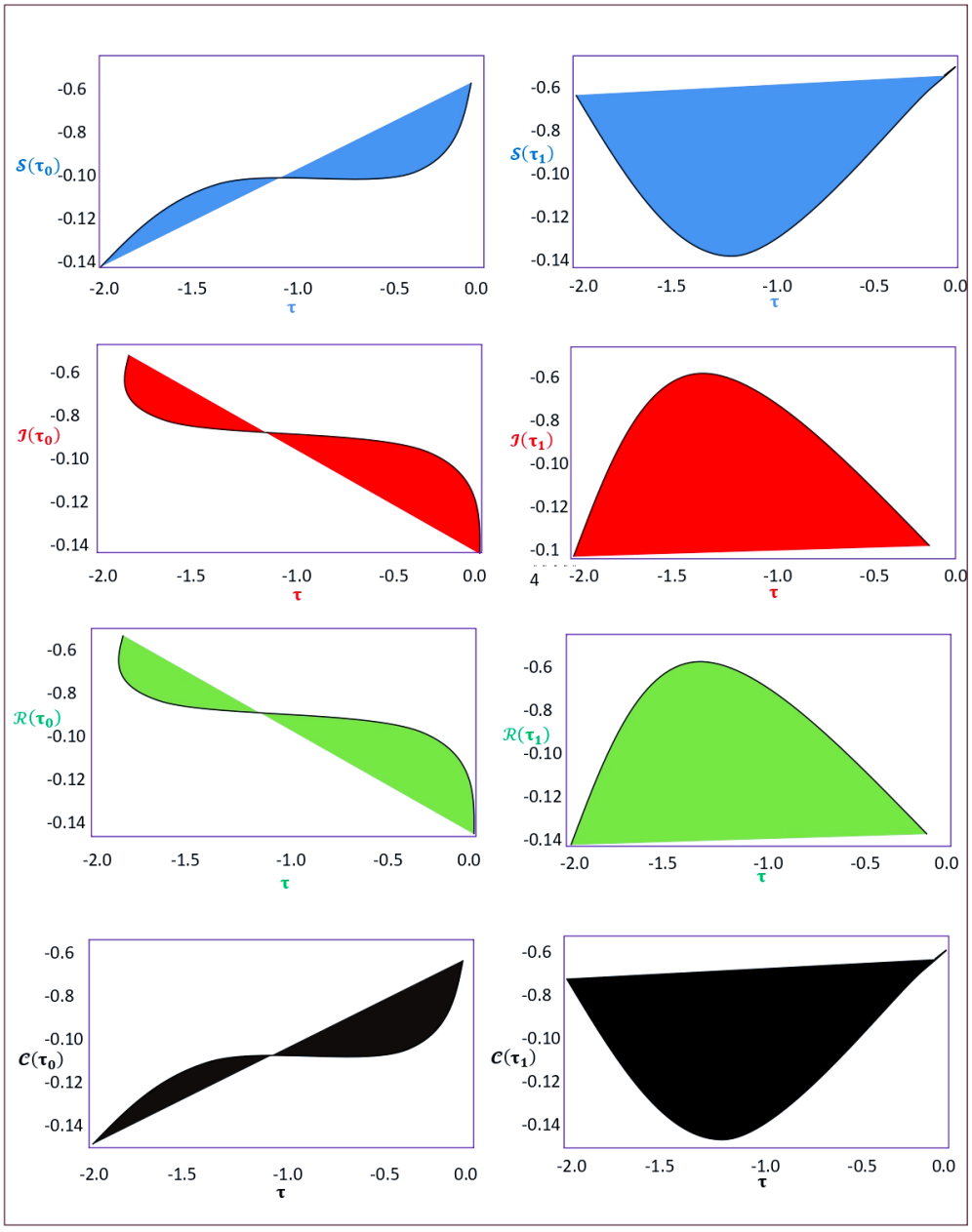

Figure 2 illustrates the comparison of the $\hbar$-curves for the fifth and sixth-order approximations of $SIRC$.

The graph $S(\tau_0)$ & $S(\tau_1)$ illustrating the comparison of the $\hbar$-curves for the fifth-order and sixth-order approximations reveals distinct convergence regions for the susceptible population. Specifically, the sixth-order approximation demonstrates a smoother and more consistent $\hbar$-curve, suggesting enhanced control over the convergence of the solution compared to the fifth-order approximation. The graph $I(\tau_0)$ & $I(\tau_1)$ represents the $\hbar$-curves for the infected population under the fifth-order and sixth-order approximations. The $\hbar$-curve for the sixth-

Received: August 05, 2025

International Journal of Applied Mathematics
Volume 38 No. 11s, 2025
ISSN: 1311-1728 (printed version); ISSN: 1314-8060 (on-line version)

order approximation is more refined with smaller fluctuations. This indicates that the sixth-order approximation provides a more reliable solution compared to the fifth-order. The graph $R(\tau_0)$ & $R(\tau_1)$shows the $\hbar$-curves for the recovered population using the fifth-order and sixth-order approximations. The sixth-order approximation yields a more stable $\hbar$-curve with minimal error regions, suggesting improved accuracy in modelling the recovery dynamics. The graph $C(\tau_0)$ & $C(\tau_1)$ depicts the $\hbar$-curves for the cross-immune population under the fifth-order and sixth-order approximations. The sixth-order approximation provides a smoother and broader convergence range, while the fifth-order approximation shows slightly less consistency. These curves show how the horizontal axis creates a legitimate "$\hbar$." The pertinent regions are listed in Table 2. An error analysis is performed in order to identify the ideal values for $\hbar$. Equations (15) through (18) can be inserted into (1) to produce the necessary residual functions.

$$\underline{E\zeta}_{(S,I,R,C)(\tau_1)}(\hbar_1) = \left(x\alpha D\left(S^{\xi}(\tau)(\hbar_1)\right) - \chi(1-S) + \varphi\left(S^{\xi}I^{\xi}(\tau)(\hbar_1)\right) - \delta\left(C^{\xi}(\tau)(\hbar_1)\right)\right) \quad (19)$$

$$\underline{E\zeta}_{(S,I,R,C)(\tau_1)}(\hbar_2) = \left(x\alpha D\left(I^{\xi}(\tau)(\hbar_2)\right) - \varphi\left(S^{\xi}I^{\xi}(\tau)(\hbar_2)\right) - \eta\varphi\left(C^{\xi}I^{\xi}(\tau)(\hbar_2)\right) + (\chi+\varphi)\left(I^{\xi}(\tau)(\hbar_2)\right)\right) \quad (20)$$

$$\underline{E\zeta}_{(S,I,R,C)(\tau_1)}(\hbar_3) = \left(x\alpha D\left(R^{\xi}(\tau)(\hbar_3)\right) - (1-\eta)\varphi\left(C^{\xi}I^{\xi}(\tau)(\hbar_3)\right) - \varphi\left(C^{\xi}(\tau)(\hbar_3)\right) + (\chi+\phi)\left(C^{\xi}(\tau)(\hbar_3)\right)\right) \quad (21)$$

$$\underline{E\zeta}_{(S,I,R,C)(\tau_1)}(\hbar_4) = \left(x\alpha D\left(R^{\xi}(\tau)(\hbar_4)\right) - \varphi\left(C^{\xi}I^{\xi}(\tau)(\hbar_4)\right) - (\chi+\delta)\left(C^{\xi}(\tau)(\hbar_4)\right) + \phi\left(R^{\xi}(\tau)(\hbar_4)\right)\right) \quad (22)$$

The expected errors are displayed for each t in (0, 1) in Table 3. This suggests that the HAM provides a near approximation to the solution of the $SIRC$ model (1). Figures 3-6 show the residual errors of τ in (0, 1) and different "α".

Table 3: The residual errors $\underline{E\zeta}_{(S,I,R,C)(\tau_1)}(\hbar)$for various, $\tau\in(0,1)$

τ	$\underline{E\zeta}_{(S,I,R,C)(\tau_1)}(\hbar_1)$	$\underline{E\zeta}_{(S,I,R,C)(\tau_1)}(\hbar_2)$	$\underline{E\zeta}_{(S,I,R,C)(\tau_1)}(\hbar_3)$	$\underline{E\zeta}_{(S,I,R,C)(\tau_1)}(\hbar_4)$
0	9.05773×10^{-7}	9.58597×10^{-9}	9.14248×10^{-8}	2.30479×10^{-9}
0.1	1.52525×10^{-6}	5.94778×10^{-9}	1.69604×10^{-7}	8.5875×10^{-8}
0.2	7.34594×10^{-6}	6.4794×10^{-6}	5.70379×10^{-7}	3.30688×10^{-6}

International Journal of Applied Mathematics
Volume 38 No. 11s, 2025
ISSN: 1311-1728 (printed version); ISSN: 1314-8060 (on-line version)

0.3	3.06653×10^{-6}	3.89008×10^{-5}	2.02822×10^{-6}	1.80537×10^{-5}
0.4	5.53734×10^{-5}	1.19367×10^{-4}	1.20506×10^{-5}	5.20511×10^{-5}
0.5	1.66688×10^{-4}	2.54236×10^{-4}	3.24383×10^{-5}	1.03328×10^{-4}
0.6	3.26493×10^{-4}	4.1493×10^{-4}	6.11003×10^{-5}	1.53968×10^{-4}
0.7	4.74678×10^{-4}	5.24149×10^{-4}	8.70219×10^{-5}	1.71343×10^{-4}
0.8	4.78428×10^{-4}	4.52458×10^{-4}	8.63747×10^{-5}	1.20174×10^{-4}
0.9	1.09547×10^{-4}	2.87077×10^{-5}	1.88407×10^{-5}	1.26712×10^{-4}
1	9.76499×10^{-4}	9.33951×10^{-4}	1.75798×10^{-4}	1.80173×10^{-4}

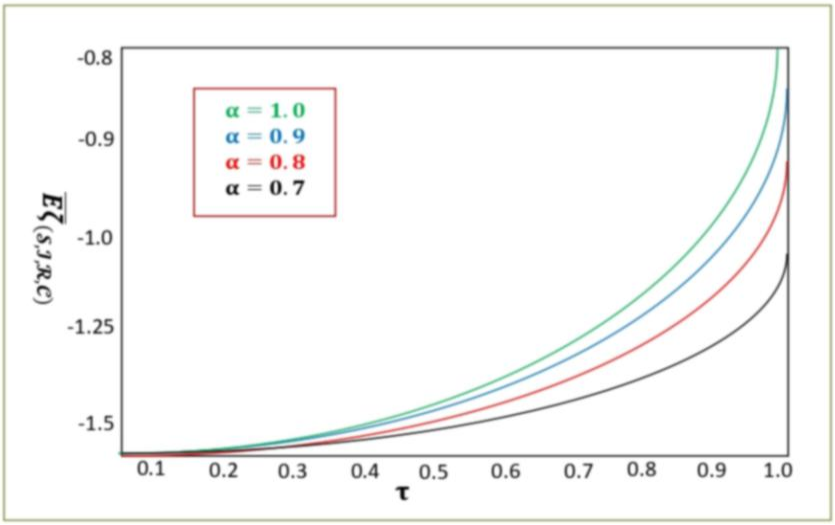

Figure 3: The behaviour of susceptible individuals (τ) with respect to time when α changes

Received: August 05, 2025

International Journal of Applied Mathematics
Volume 38 No. 11s, 2025
ISSN: 1311-1728 (printed version); ISSN: 1314-8060 (on-line version)

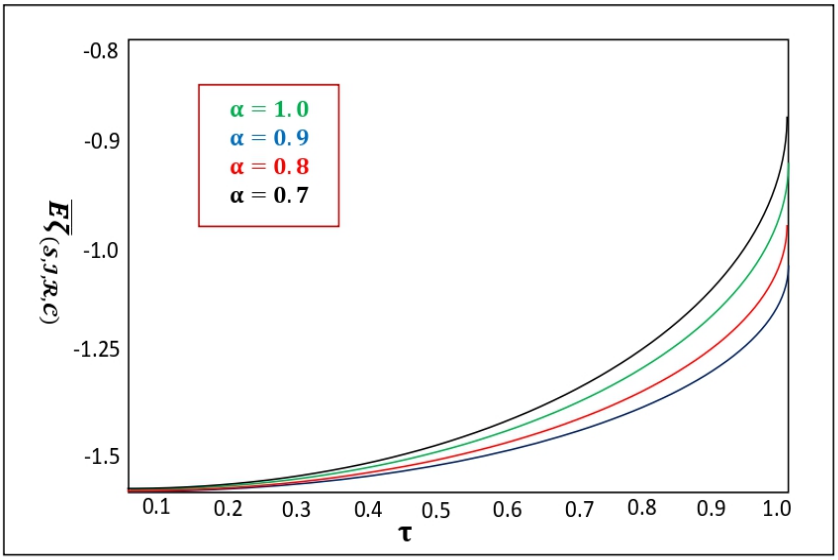

Figure 4: The behaviour of infected individuals (τ) with regard to time when α changes.

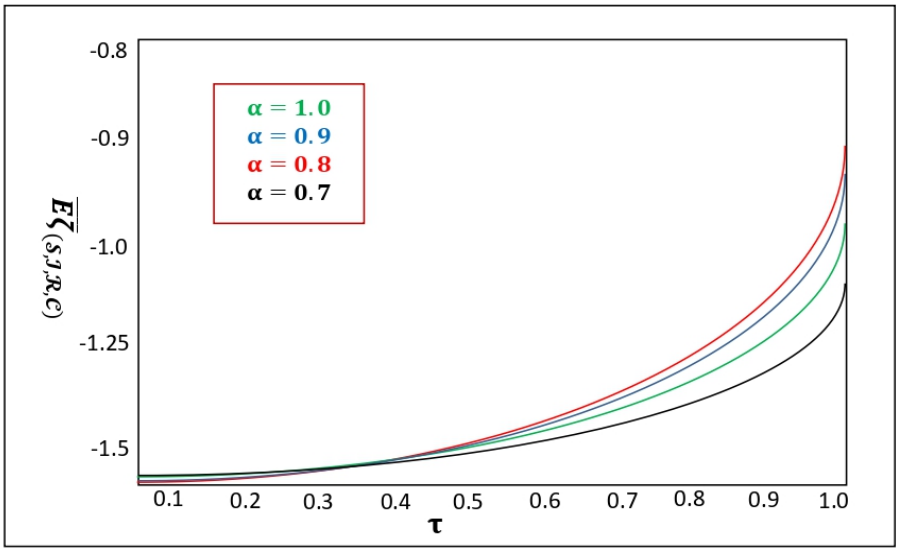

Figure 5: The behaviour of recovered individual (τ) with regard to time when α changes.

Received: August 05, 2025

International Journal of Applied Mathematics
Volume 38 No. 11s, 2025
ISSN: 1311-1728 (printed version); ISSN: 1314-8060 (on-line version)

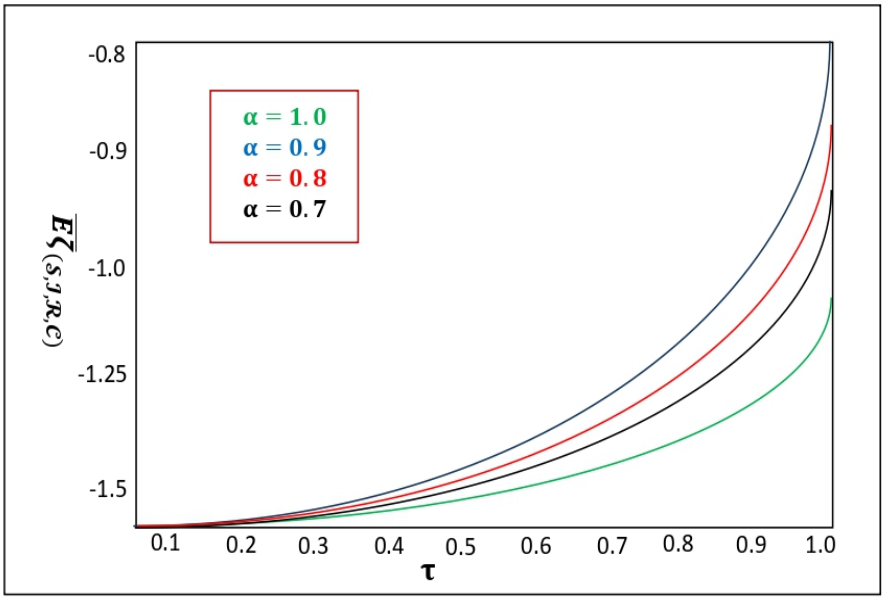

Figure 6: The behaviour of cross immune individuals $C(\tau)$ with regard to time when α changes.

This ensures that the method reliably captures the dynamics of individuals transitioning between immunity states. Based on the following 6th order approximation, we estimate the square residual error to be

$$\underline{\zeta}_{S(\tau_1)}(\hbar_1) = \int_0^1 \left(\underline{E\zeta}_{(S,I,R,C)(\tau_1)}(\hbar_1)\right)^2 d\tau \tag{23}$$

$$\underline{\zeta}_{I(\tau_1)}(\hbar_2) = \int_0^1 \left(\underline{E\zeta}_{(S,I,R,C)(\tau_1)}(\hbar_2)\right)^2 d\tau \tag{24}$$

$$\underline{\zeta}_{R(\tau_1)}(\hbar_3) = \int_0^1 \left(\underline{E\zeta}_{(S,I,R,C)(\tau_1)}(\hbar_3)\right)^2 d\tau \tag{25}$$

$$\underline{\zeta}_{C(\tau_1)}(\hbar_4) = \int_0^1 \left(\underline{E\zeta}_{(S,I,R,C)(\tau_1)}(\hbar_4)\right)^2 d\tau \tag{26}$$

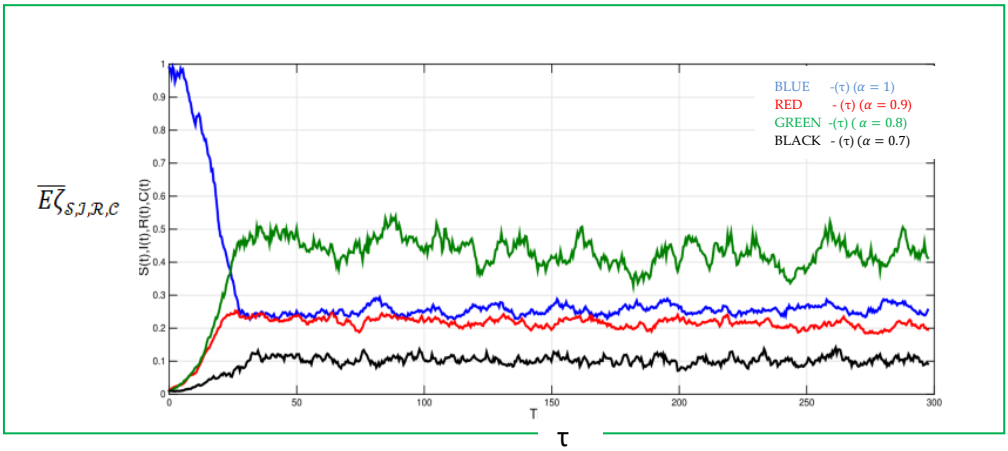

Figure 7: $SIRC$ epidemic model with a therapeutic cure rate

Received: August 05, 2025

International Journal of Applied Mathematics
Volume 38 No. 11s, 2025
ISSN: 1311-1728 (printed version); ISSN: 1314-8060 (on-line version)

By altering α for every biological class (Susceptible, Infected, Recovered, and Cross-immune), we may accurately take into consideration variations in the ways that previous states affect each population group's future development.

Values of $\hbar_1, \hbar_2, \hbar_3$ and $\hbar_4$ for which $\underline{\zeta}_{S(\tau_1)}(\hbar_1)$, $\underline{\zeta}_{I(\tau_1)}(\hbar_2), \underline{\zeta}_{R(\tau_1)}(\hbar_3)$, $\underline{\zeta}_{C(\tau_1)}(\hbar_4)$ are minimum can be obtained. Thus we have $x\alpha D\underline{\zeta}_{S(\tau_1)}({\hbar_1}^*) = 0$, $x\alpha D\underline{\zeta}_{I(\tau_1)}({\hbar_2}^*) = 0$, $x\alpha D\underline{\zeta}_{R(\tau_1)}({\hbar_3}^*) = 0$, $x\alpha D\underline{\zeta}_{C(\tau_1)}({\hbar_4}^*) = 0$.

The optimal values $\hbar_1$, $\hbar_2$, $\hbar_3$ & $\hbar_4$ for all of the cases considered are obtained as $({\hbar_1}^*) = -0.856097, ({\hbar_2}^*) = -1.0557, ({\hbar_3}^*) = -0.913549, ({\hbar_4}^*) = -1.04116$. For the ideal values of $\hbar_1$, $\hbar_2$, $\hbar_3$ and $\hbar_4$, Table 4 displays the minimum values of $\underline{\zeta}_{S(\tau_1)}(\hbar_1)$, $\underline{\zeta}_{I(\tau_1)}(\hbar_2), \underline{\zeta}_{R(\tau_1)}(\hbar_3)$, $\underline{\zeta}_{C(\tau_1)}(\hbar_4)$.

Table 4: The minimum values of, $\underline{\zeta}_{S(\tau_1)}({\hbar_1}^*), \underline{\zeta}_{I(\tau_1)}({\hbar_2}^*), \underline{\zeta}_{R(\tau_1)}({\hbar_3}^*), \underline{\zeta}_{C(\tau_1)}({\hbar_4}^*)$ (see Figure 8)

$\hbar^*$	**Minimum value**
$\underline{\zeta}_{S(\tau_1)}(\hbar_1)$	$-0.856097 \leq \hbar_1 \leq 8.38046 \times 10^{-8}$
$\underline{\zeta}_{I(\tau_1)}(\hbar_2)$	$-1.0557 \leq \hbar_2 \leq 9.75647 \times 10^{-8}$
$\underline{\zeta}_{R(\tau_1)}(\hbar_3)$	$-0.913549 \leq \hbar_3 \leq 2.79827 \times 10^{-9}$
$\underline{\zeta}_{C(\tau_1)}(\hbar_4)$	$-1.04116 \leq \hbar_4 \leq 9.28625 \times 10^{-9}$

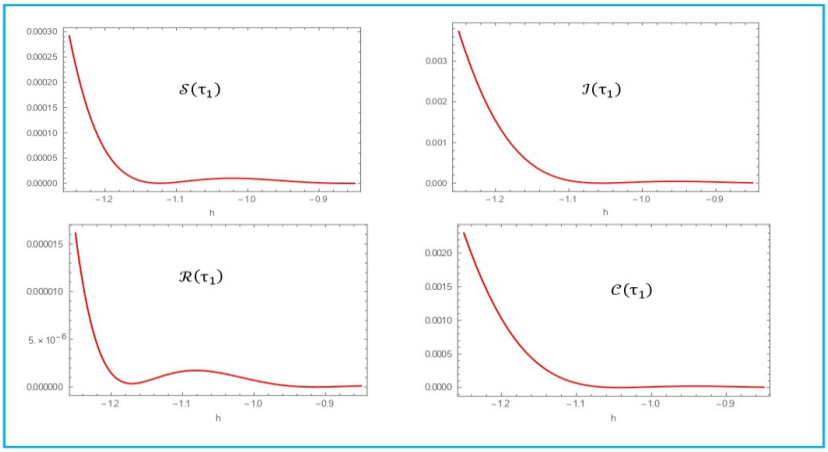

Figure 8: Minimum and maximum values of $S(\tau_1)$, $I(\tau_1)$, $R(\tau_1)$, $C(\tau_1)$

The present analysis reveals that the fractional order parameter α plays a crucial role in determining the dynamical behavior of the epidemic model. Biologically, a decrease in the fractional order (α<1) signifies a stronger memory effect in the system, implying that the future evolution of each population class—susceptible, infected, recovered, and cross-immune—

Volume 38 No. 11s, 2025
ISSN: 1311-1728 (printed version); ISSN: 1314-8060 (on-line version)

depends more heavily on their historical states. This memory property results in delayed infection peaks and prolonged persistence of the disease, reflecting realistic epidemic scenarios where individuals' immune responses and behavioral changes do not occur instantaneously. Conversely, when α\alphaα approaches unity, the model behavior tends toward that of the classical integer-order system, leading to faster epidemic oscillations and shorter infection durations. Hence, the fractional-order framework offers a more flexible and biologically accurate representation of the disease transmission process by capturing the hereditary and immune memory effects often ignored in conventional models.

The inclusion of cross-immunity and therapeutic cure rate further enhances the biological realism of the proposed $SIRC$ model. The cross-immune compartment reflects individuals who, after recovery, retain partial immunity that reduces their susceptibility to reinfection. The results indicate that a higher cross-immunity rate slows down the overall spread of infection and stabilizes the system, thereby lowering the infection prevalence over time. Similarly, the therapeutic cure rate introduces a dynamic recovery mechanism that effectively decreases the infectious population, aligning with medical interventions such as antiviral treatments or vaccination campaigns. These results underline the importance of incorporating post-recovery immunity and treatment strategies in fractional epidemic models for improved epidemiological forecasting.

Comparing the current findings with previous works provides additional insight into the model's novelty and impact. For instance, Verma et al. [41] investigated a fractional-order SIR–SI model for dengue fever using Caputo derivatives, emphasizing the role of memory effects in disease persistence. However, their framework did not include cross-immunity or treatment effects, which are vital for realistic modeling of post-infection immunity. In contrast, Alshammari et al. [42] applied a fractional SEIR model for measles transmission under the Caputo operator, achieving accurate numerical solutions through hybrid analytical techniques but without explicit convergence control. The present work extends these contributions by employing the Homotopy Analysis Method (HAM)**,** which offers explicit convergence management through h-curves and provides analytical approximations requiring only six terms for high precision. This combination of Caputo–Fabrizio derivative and HAM-based solution not only ensures computational efficiency but also establishes a new analytical framework for modeling infectious diseases with memory, treatment, and partial immunity effects.

7. CONCLUSION

This study develops a fractional-order $SIRC$ epidemic model that integrates cross-immunity and therapeutic interventions, providing a biologically realistic framework for analyzing infectious disease dynamics. By employing the Homotopy Analysis Method (HAM) with Caputo–Fabrizio derivatives, the model achieves accurate analytical approximations with efficient convergence control. The results demonstrate that incorporating memory effects and treatment significantly influences infection persistence and recovery behavior. This highlights the importance of considering fractional-order dynamics when designing public health strategies such as vaccination and therapy optimization. The proposed approach not only

Received: August 05, 2025

Volume 38 No. 11s, 2025
ISSN: 1311-1728 (printed version); ISSN: 1314-8060 (on-line version)

improves analytical precision but also strengthens the link between mathematical modeling and real-world epidemiology. Future work can extend this framework to include variable transmission rates, demographic changes, and stochastic effects, offering deeper insight into the complex interplay between immunity, treatment, and disease propagation.

REFERENCES

[1]. Xavier JB, Monk JM, Poudel S, et al. Mathematical models to study the biology of pathogens and the infectious diseases they cause. iScience. 2022;25(4):104079. http://dx.doi.org/10.1016/j.isci.2022.104079.

[2]. Sabir Z, Umar M. Levenberg-Marquardt back propagation neural network procedures for the consumption of hard water-based kidney function. Int .J .Math.Comput. Eng. 2023;1(1):127–138 http://dx.doi.org/10.2478/ijmce-2023-0010.

[3]. Tripathi A, Tripathi RN, Sharma D. A mathematical model to study the COVID-19 pandemic in India. Model Earth Syst Environ. 2022;8:3047–3058. http://dx.doi.org/ 10.1007/s40808-021-01280-8.

[4]. Cassels S, Clark SJ, Morris M. Mathematical models for HIV transmission dynamics: tools for Social and behavioral science research. JAIDS J Acquired Immune Defic Syndr. 2008;47:S34-S39. http://dx.doi.org/10.1097/QAI.0b013e3181605da3.

[5]. Goyal A, Liao LE, Perelson AS. Within-host mathematical models of hepatitis B virus infection: Past, present, and future. Curr.Opin.Syst Biol. 2019;18:27–35. http://dx.doi.org/10.1016/j.coisb.2019.10.003.

[6]. Sadki M, Harroudi S, Allali K. Local and global stability of an HCV viral dynamics model with two routes of infection and adaptive immunity. Comput Methods Biomech Biomed Eng.2023:1–28. http://dx.doi.org/10.1080/10255842. 2023.2245941.

[7]. Kermack WO, McKendrick AG. A contribution to the mathematical theory of epidemics.ProcR SocLondSer A. 1927;115(772):700–721.http://dx.doi.org/10. 1098/rspa.1927.0118.

[8]. Taylor ML, Carr TW. An SIR epidemic model with partial temporary immunity modelled with delay. J Math Biol. 2009;59:841–880. http://dx.doi.org/10.1007/ s00285-009-0256-9.

[9]. Eckalbar JC, Eckalbar WL. Dynamics of an epidemic model with quadratic treatment. Nonlinear Anal RWA. 2011;12(1):320–332. http://dx.doi.org/10.1016/ j.nonrwa.2010.06.018.

[10]. Sadki M, Harroudi S, Allali K. Dynamical analysis of an HCV model with cell-tocell transmission and cure rate in the presence of adaptive immunity. Math Model Comput. 2022;9(3):579–593. http://dx.doi.org/10.23939/mmc2022.03.579.

[11]. Hethcote HW. Qualitative analyses of communicable disease models. Math Biosci.1976;28(3–4):335–356. http://dx.doi.org/10.1016/0025-5564(76)90132-2.

Received: August 05, 2025

Volume 38 No. 11s, 2025
ISSN: 1311-1728 (printed version); ISSN: 1314-8060 (on-line version)

[12]. Yusuf TT, Benyah F. Optimal control of vaccination and treatment for an SIR epidemiological model. World J Model Simul. 2012;8(3):194–204.
[13]. Lahrouz A, El Mahjour H, Settati A, Bernoussi A. Dynamics and optimal control of a non-linear epidemic model with relapse and cure. Physica A. 2018;496:299–317. http://dx.doi.org/10.1016/j.physa.2018.01.007.
[14]. Muroya Y, Li H, Kuniya T. Complete global analysis of an SIRS epidemic model with graded cure and incomplete recovery rates. J Math Anal Appl. 2014;410(2):719-732. http://dx.doi.org/10.1016/j.jmaa.2013.08.024.
[15]. Muroya Y, Kuniya T. Global stability for a delayed multi-group SIRS epidemic model with cure rate and incomplete recovery rate. Int J Biomath. 2015;8(04):1550048. http://dx.doi.org/10.1142/S1793524515500485.
[16]. Ross B. The development of fractional calculus 1695–1900.Historia Math. 1977;4(1):75–89.
http://dx.doi.org/10.1016/0315-0860(77)90039-8.
[17]. Podlubny I. Fractional Differential Equations: An Introduction to Fractional Derivatives, Fractional Differential Equations, To Methods of their Solution and Some of their Applications.Elsevier; 1998.
[18]. Atangana A, Baleanu D. New fractional derivatives with nonlocal and non-singular kernel: theory and application to heat transfer model. 2016 http://dx.doi.org/10. 48550/arXiv.1602.03408, arXiv preprint arXiv:1602.03408.
[19]. Caputo M, Fabrizio M. A new definition of fractional derivative without singular kernel. ProgrFract Differ Appl. 2015;1(2):73–85. http://dx.doi.org/10.12785/pfda/ 010201.
[20]. Defterli O, Baleanu D, Jajarmi A, Sajjadi SS, Alshaikh N, Asad J. Fractional treatment: an accelerated mass-spring system. Romanian Rep Phys. 2022;74(4):1–13.
[21]. Jajarmi A, Baleanu D, Sajjadi SS, Nieto JJ. Analysis and some applications of a regularized ψ–Hilfer fractional derivative.JComputAppl Math. 2022;415:114476. http://dx.doi.org/10.1016/j.cam.2022.114476.
[22]. Huo J, Zhao H, Zhu L. The effect of vaccines on backward bifurcation in a fractional order HIV model. Nonlinear Anal RWA. 2015;26:289–305. http://dx.doi.org/10.1016/j.nonrwa.2015.05.014.
[23]. Baleanu D, Jajarmi A, Mohammadi H, Rezapour S. A new study on the mathematical modelling of human liver with Caputo–Fabrizio fractional derivative. Chaos Solitons Fractals. 2020;134:109705.
http://dx.doi.org/10.1016/j.chaos.2020. 109705.
[24]. Sadki M, Danane J, Allali K. Hepatitis c virus fractional-order model: mathematical analysis. Model Earth Syst Environ. 2022. http://dx.doi.org/10.1007/s40808-022- 01582-5.
[25]. Ahmad S, Ullah A, Akgül A, Al Bayatti H. Theoretical Analysis of HBV Infection Under Mittag-Leffler Derivative. Progr. Fract. Differ. Appl. 9; 2023;1;99-106. http://dx.doi.org/10.18576/pfda/090107.

Received: August 05, 2025

Volume 38 No. 11s, 2025
ISSN: 1311-1728 (printed version); ISSN: 1314-8060 (on-line version)

[26]. Rezapour S, Mohammadi H, Samei ME. SEIR epidemic model for COVID-19 transmission by Caputo derivative of fractional order. Adv Differ Equ. 2020;2020:490. http://dx.doi.org/10.1186/s13662-020-02952-y.

[27]. Paul S, Mahata A, Mukherjee S, Roy B. Dynamics of SIQR epidemic model with fractional order derivative. Partial Differ EquAppl Math. 2022;5:100216. http://dx.doi.org/10.1016/j.padiff.2021.100216.

[28]. Khalaf SL, Kadhim MS, Khudair AR. Studying of COVID-19 fractional model: Stability analysis. Partial Differ EquAppl Math. 2023;7:100470. http://dx.doi.org/ 10.1016/j.padiff.2022.100470.

[29]. Akdim K, Ez-Zetouni A, Zahid M. The influence of awareness campaigns on the spread of an infectious disease: a qualitative analysis of a fractional epidemic model. Model Earth SystEnviron. 2021;8:1311–1319.
http://dx.doi.org/10.1007/ s40808-021-01158-9.

[30]. Bounkaicha C, Allali K. Dynamics of a time fractional order spatio-temporal SIR with vaccination and temporary immunity. Partial Differ EquAppl Math. 2023;7:100524. http://dx.doi.org/10.1016/j.padiff.2023.100524.

[31]. Pandey HR, Phaijoo GR, Gurung DB. Vaccination effect on the dynamics of dengue disease transmission models in nepal: A fractional derivative approach. Partial Differ EquApplMath. 2023;7:100476.
http://dx.doi.org/10.1016/j.padiff. 2022.100476.

[32]. Jafari H, Goswami P, Dubey R, Sharma S, Chaudhary A. Fractional SZIR model of zombies infection. 2022. http://dx.doi.org/10.22541/au.165294204.44635425/ v1.

[33]. Barros LCd, Lopes MM, Pedro FS, Esmi E, Santos JPCd, Sánchez DE. The memory effect on fractional calculus: an application in the spread of COVID-19. ComputAppl Math.2021;40(3):72.
http://dx.doi.org/10.1007/s40314-021-01456-z.

[34]. AllaHamou A, Azroul E, LamraniAlaoui A. Fractional model and numerical algorithms for predicting COVID-19 with isolation and quarantine strategies. Int J ApplComput Math.2021;7(4):142. http://dx.doi.org/10.1007/s40819-021-01086- 3.

[35]. Qureshi S. Periodic dynamics of rubella epidemic under standard and fractional Caputo operator with real data from Pakistan. 2020:151–165. 178, http://dx.doi. org/10.1016/j.matcom.2020.06.002.

[36]. Singh R, Mishra J, Gupta VK. The dynamical analysis of a tumor growth model under the effect of fractal fractional Caputo-Fabrizio derivative. Int J Math Comput Eng. 2023.http://dx.doi.org/10.2478/ijmce-2023-0009.

[37]. Jajarmi A, Ghassabzade FA. Optimal Control and General Fractional Description for a Complex Biological System.Progr. Fract. Differ. Appl. 9; 2023; 3; 389-396.http://dx.doi.org/10.18576/pfda/090304.

[38]. Dos Santos JC, Monteiro E, Vieira GB. Global stability of fractional SIR epidemic model. (1). 2017. In: Proceeding Series of the Brazilian Society of Computational and Applied Mathematics; Vol. 5,
http://dx.doi.org/10.5540/03.2017.005. 01.0019.

Received: August 05, 2025

Volume 38 No. 11s, 2025
ISSN: 1311-1728 (printed version); ISSN: 1314-8060 (on-line version)

[39]. Veeresha P, Ilhan E, Prakasha D, Baskonus HM, Gao W. A new numerical investigation of fractional order susceptible-infected-recovered epidemic model of childhood disease. Alex Eng J. 2022;61(2):1747–1756. http://dx.doi.org/10.1016/ j.aej.2021.07.015.

[40]. Alzahrani. Statistical methods for the computation and parameter estimation of a fractional SIRC model with salmonella infection. Heliyon, 10(10), 2024, 2405-8440. https://doi.org/10.1016/j.heliyon.2024.e30885.

[41]. Verma, Lalchand, Ramakanta Meher, Omid Nikan, and Akeel A. Al-Saedi. Numerical study on fractional order nonlinear SIR-SI model for dengue fever epidemics.Scientific Reports 15, no. 1 (2025): 30677. https://doi.org/10.1038/s41598-025-16599-w.

[42].Alshammari, Nawa A., N. S. Alharthi, Abdulkafi Mohammed Saeed, Adnan Khan, and Abdul Hamid Ganie. Numerical solutions of a fractional order SEIR epidemic model of measles under Caputo fractional derivative. PloS one 20, no. 5 (2025): e0321089 . https:// doi.org/10.1371/journal.pone.0321089.

Received: August 05, 2025